ELSEVIER

Contents lists available at ScienceDirect

Redox Biology

journal homepage: www.elsevier.com/locate/redox



Alleviation of accelerated diabetic atherogenesis in STZ-treated apoE/NOX1 DKO mice, apoE^{-/-}/tg-EC-DHFR mice, and by folic acid

Yixuan Zhang, Ji Youn Youn, Kai Huang, Yuhan Zhang, Hua Cai * 🗅

Division of Molecular Medicine, Department of Anesthesiology, Division of Cardiology, Department of Medicine, David Geffen School of Medicine, University of California Los Angeles, California, 90095, USA

ARTICLEINFO

Keywords:
Diabetes
Atherosclerosis
Diabetic atherogenesis
Dihydrofolate reductase (DHFR)
Endothelial-specific DHFR transgenic mice (tg-EC-DHFR)
Endothelial nitric oxide synthase (eNOS) uncoupling
apoE null mice (apoE^{-/-})
NADPH oxidase isoform 1 (NOX1)
NOX1 knockout mice (apoE^{-/-}/NOX1^{-/y})
apoE/NOX1 double knockout mice (apoE^{-/-}/NOX1^{-/y})

ABSTRACT

We and others have previously shown that uncoupling of endothelial nitric oxide synthase (eNOS) induces oxidative stress in diabetes, contributing to endothelial dysfunction. Activation of NADPH oxidase (NOX) isoform NOX1 by angiotensin II (Ang II) triggers eNOS uncoupling via deficiency in dihydrofolate reductase (DHFR) in streptozotocin (STZ)-induced type 1 diabetic mice. Presently, we investigated whether accelerated atherosclerosis is attenuated in apoE/NOX1 double knockout, and whether mice overexpressing DHFR in the endothelium (tg-EC-DHFR, generated in house) recouples eNOS to alleviate diabetic atherogenesis. At baseline, endothelialspecific DHFR overexpression recoupled eNOS and improved vasorelaxation in the aortas and mesenteric arteries of STZ-induced diabetic mice. Accelerated atherogenesis in STZ/high-fat diet (HFD) treated apoE^{-/-} was markedly abrogated in tg-EC-DHFR background, establishing an important role of endothelial DHFR in maintaining vascular function and protecting from diabetic atherogenesis. Moreover, by crossing apoE^{-/-} with NOX1 null mice (NOX1-'y), we found that NOX1 deletion markedly diminished atherosclerotic lesion formation in HFD + STZ-treated apoE^{-/-}/NOX1^{-/y} mice, indicating that NOX1 lies upstream of eNOS uncoupling in facilitating diabetic atherogenesis. Oral administration with folic acid (FA), shown to upregulate DHFR, robustly attenuated atherosclerotic lesion formation in HFD + STZ-treated apo $E^{-/-}$ mice similarly to NOX1 deletion. Taken together, our data for the first time demonstrate that endothelial DHFR plays an important role in the preservation of endothelial function and inhibition of atherosclerosis in diabetes, deficiency of which consequent to NOX1 activation mediates eNOS uncoupling driven lesion formation. Strategies targeting uncoupled eNOS prove to be robust treatment options for diabetic endothelial dysfunction and atherogenesis.

1. Introduction

Endothelial dysfunction attributed to increased oxidative stress has been implied in the pathogenesis of cardiovascular complications in diabetes. We and others have previously shown that uncoupled endothelial nitric oxide synthase (eNOS) represents the major source of continuous production of reactive oxygen species (ROS) in both type 1 diabetes mellitus (T1DM) and type 2 diabetes mellitus (T2DM), contributing to vascular dysfunction and consequent atherogenesis [1–8]. We have previously demonstrated that eNOS uncoupling develops in STZ-induced T1DM in response to elevated angiotensin II (Ang II) levels [1,3], while it is activated by a bone morphogenic protein (BMP)-4-dependent mechanism in T2DM [5,7]. Specifically, eNOS uncoupling is induced by Ang II-dependent activation of NADPH oxidase (NOX) in streptozotocin (STZ)-induced type 1 diabetic mice [1,3,9]. We

have previously discovered that exposure of endothelial cells to Ang II, known to be elevated in patients with T1DM, leads to transient activation of NOX triggering hydrogen peroxide production and hydrogen peroxide-mediated dihydrofolate reductase (DHFR) deficiency, resulting in consequent uncoupling of eNOS [9]. These data indicate that eNOS uncoupling is the primary enzymatic source of sustained vascular ROS production in T1DM. In the present study we aimed to investigate whether several strategies inactivating upstream mediators of eNOS uncoupling, is protective of accelerated atherogenesis in T1DM.

It has been well recognized that normal function of eNOS production of nitric oxide (NO) is essential to maintain vascular homeostasis to prevent diabetic vascular dysfunction and complications. Under pathological conditions when eNOS cofactor tetrahydrobiopterin (H_4B) is deficient due to oxidative inactivation following NOX-derived ROS production, eNOS becomes uncoupled to function as a pro-oxidant

E-mail address: hcai@mednet.ucla.edu (H. Cai).

^{*} Corresponding author.

enzyme, producing superoxide instead of NO. Others and we have previously demonstrated that DHFR, a salvage enzyme that regenerates H₄B from its oxidized form dihydrobiopterin (H2B), is downregulated in aortas of STZ-induced T1DM mice consequent to NOX1 production of hydrogen peroxide, leading to eNOS uncoupling and endothelial dysfunction [1,3,9-15], and likewise in db/db T2DM mice [5,16,17]. These data establish an essential role of DHFR deficiency in mediating diabetic endothelial dysfunction that is anticipated to proceed accelerated atherogenesis, which is examined in the present study in the setting of endothelial specific DHFR transgenic mice. Moreover, oral administration of folic acid (FA) or systematical overexpression of DHFR, recoupled eNOS and improved endothelium-dependent vasorelaxation in STZ-injected or Ang II-infused mice [3,18], strongly indicating that restoration of DHFR function is robustly effective in alleviating diabetic endothelial dysfunction. Meanwhile, it is well established that diabetes is associated with accelerated atherogenesis, and that eNOS uncoupling is one of the causal factors of atherogenesis. Therefore, we hypothesized that endothelial-specific overexpression of DHFR using endothelial specific DHFR transgenic mice made in house, prevents endothelial dysfunction in diabetes to abrogate diabetic atherogenesis through recoupling of eNOS, which is fully investigated in the present study.

NOXs represent the major sources of ROS production during cardiovascular pathogenesis [6]. We have previously demonstrated that NOX1, but not NOX2 or NOX4, is specifically and robustly activated in diabetes [3,5], lying upstream of eNOS uncoupling and endothelial dysfunction by driving DHFR deficiency. We have also shown that genetic deletion or in vivo siRNA knockdown of NOX1 recouples eNOS to markedly restore vasorelaxation in STZ-induced diabetic mice via preservation of DHFR function [3]. Of note, knockout of NOX1 in apolipoprotein E-deficient (apoE^{-/-}) mice attenuated atherosclerosis induced by STZ injection or high-fat diet (HFD), which was found associated with reduced aortic ROS production [4,19]. However, whether NOX1 deletion attenuated atherosclerosis via recoupling eNOS has not been previously elucidated. We have previously shown that oral administration of FA robustly recouples eNOS in STZ induced diabetic mice, Ang II infused apoE null mice, Ang II infused hph-1 mice, or Fbn1^{C1039G/+} mice, resulting in alleviation of endothelial dysfunction during the processes of diabetic progression and formation of aortic aneurysms [3,10,13,14,20-23]. FA administration also significantly lowered blood pressure in Ang II infused wild type animals [13]. Therefore, we hypothesized that NOX1 deletion, or recoupling of eNOS with oral FA administration, is highly effective in attenuating accelerated atherogenesis in diabetes, as fully addressed by current experimental investigation.

For the first time in the present study, we generated in house an endothelial-specific DHFR transgenic (tg-EC-DHFR) mice to have demonstrated a protective role of endothelial DHFR overexpression in attenuating STZ-induced diabetic endothelial dysfunction and atherogenesis via recoupling of eNOS and restoration of NO bioavailability. Our data also demonstrated that NOX1-dependent eNOS uncoupling mediates development of diabetic atherogenesis since markedly diminished lesion formation in $apoE^{-/-}/NOX1^{-/y}$ double knockout mice was accompanied by recoupling of eNOS. Of note, oral administration of FA showed similar protective effects as NOX1 deletion did in STZ-treated $\mbox{apoE}^{-/-}$ mice, indicating that NOX1 and eNOS uncoupling aligns in the same axis in mediating acceleration of diabetic atherogenesis. These results illustrate an innovative and central role of endothelial specific DHFR targeting as a robust therapeutic strategy for treating diabetic endothelial dysfunction and accelerated atherogenesis, and a previously uncovered NOX1/eNOS uncoupling axis in the development of diabetic atherogenesis that can also be targeted by NOX1 deletion or FA administration. Our data therefore demonstrate that targeting NOX1, endothelial DHFR deficiency or eNOS uncoupling can be used to develop novel and robust therapeutic regimes for the management of diabetic vascular dysfunction and atherosclerotic complications.

2. Methods

2.1. Generation of endothelial-specific DHFR transgenic mice

The full coding region of the mouse DHFR gene (NM_010049) was purchased from OriGene (#MC203752) and subcloned into pSTEC-1 plasmid (a generous gift from Dr. Curt Sigmund, Medical College of Wisconsin, Milwaukee) [24]. The sequence encoding an HA tag was introduced to the N-terminus of DHFR gene by PCR (KOD Hot Start DNA Polymerase, #71086, MilliporeSigma, Burlington, MA) with forward primer 5'-AAAGCTAGCATGTACCCATACGATGTTCCAGATTACGCTAT GGTTCGTCACCATT-3' and reverse primer 5'-TTTGCGGCCGCTTAG TCTTTCTTCTGT-3'. Then, the fragment containing Intron-HA-DHFR-polyA was subcloned into pBS-ve-LacZ vector (Fig. 1A), which contains an endothelial-specific Ve-Cadherin promoter. The final construct was sequenced before linearization and microinjection into fertilized C57BL/6 mouse embryos at the Transgenic Mouse Facility at University of California, Irvine.

Two pairs of genotyping primers were designed to distinguish transgenic (tg-EC-DHFR) from wild type (WT) littermates (Fig. 1B). One pair of primers was designed on exon 1 and 2 (spanning intron 1) (forward primer, F1: 5'-GGTTCGACCATTGAACTGCATCGTC-3'; reverse primer, R1: 5'-CCACTGAAGAGGTTGTGGTCATTCT-3'), and generated a product of 440 bp and 131 bp from WT and tg-EC-DHFR mice, respectively (Fig. 1B). The other pair of genotyping primers was designed to target HA tag in the transgenic construct (forward primer, F2: 5'-CCCATACGATGTTCCAGATTACG-3'; reverse primer, R2: 5'-ACA-GAACTGCCTCCGACTATCCA-3') with a PCR product of 387 bp in tg-EC-DHFR animals, but no product from WT animals (Fig. 1B).

Fourteen viable founders were generated from the microinjection. We next crossed each founder with WT C57BL/6 animals to produce F1 generation. WT and tg-EC-DHFR F1 generation were born at a normal Mendelian ratio and showed no obvious abnormality. We harvested aortic tissue from F1 generation to examine expression of DHFR in WT and tg-EC-DHFR littermates by Western blot. At least two litters of F1 generation were harvested from each founder. We found that F1 generation from founder #6-1 (Fig. 1C) and #73-7 (Suppl. Fig. 1A) showed stable and consistent overexpression of DHFR in the aortas. No difference in body weight and organ weights was found between WT and tg-EC-DHFR littermates (Suppl. Fig. 1B, Suppl. Fig. 3). Both WT and tg-EC-DHFR offspring from founder #6-1 and #73-7 showed similar response to streptozotocin (STZ, #S0130, MilliporeSigma, Burlington, MA) with elevated fasting glucose levels in the plasma (Fig. 3, Suppl. Fig. 2). For the rest of the experiments, offsprings from founder #6-1 were used.

2.2. Generation of double knockout strains of apoE $^{-/-}$ /tg-EC-DHFR and apoE $^{-/-}$ /NOX1 $^{-/y}$

All animals and experimental procedures were approved by the Institutional Animal Care and Usage Committee at the University of California, Los Angeles. Breeders of apolipoprotein E-deficient (apoE^{-/} -) mice were purchased from Jackson Laboratory (#002052, Bar Harbor, ME). Some of the apoE null mice were crossed with tg-EC-DHFR mice to generate apoE^{-/-}/tg-EC-DHFR animals. Breeders of NOX1 null (NOX1 gene is X-chromosome located) mice were generously provided by Dr. Karl-Heinz Krause from the University of Geneva [3,25]. Double knockout mice of NOX1 and apoE were generated in house. NOX1 null mice (X chromosome linked) were bred with apo $E^{-/-}$ to generate females with genotype of apoE^{-/-}/NOX1^{+/-}. Then apoE^{-/-}/NOX1^{+/-} females were bred with apoE^{-/-} males to generate male offspring littermates with genotypes of apoE^{-/-}/NOX1^{-/y} and $apoE^{-/-}/NOX1^{+/y}$. Animals were maintained specific-pathogen-free, temperature-controlled facility on a 12:12-h light/dark cycle with ad libitum access to food and water.

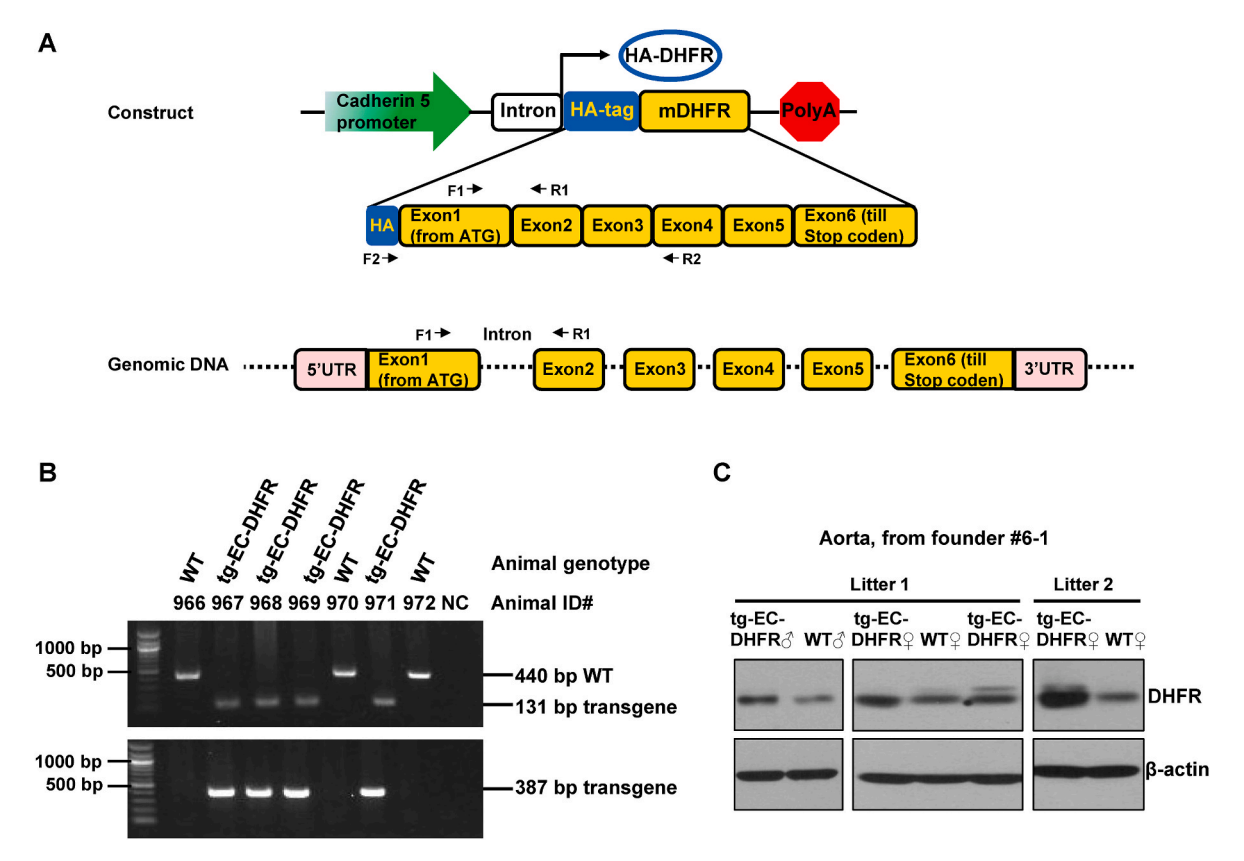


Fig. 1. Generation of endothelial-specific DHFR transgenic mice. **(A)** Illustration of linearized DNA fragment for production of endothelial-specific DHFR transgenic mice (tg-EC-DHFR). Coding region of mouse DHFR gene was cloned with HA-tag into a construct driven by Cadherin 5 promoter. Two sets of genotyping primer were designed to distinguish tg-EC-DHFR mice from wild type (WT) animals. Primers F1 and R1 were designed to target exon 1 and exon 2 (cross intron) to separately amplify DNA fragment for the endogenous gene (product at 440 bp) or DHFR transgene (product at 131 bp). Primers F2 and R2 were designed to identify the presence of HA-tag (product at 387 bp). mDHFR: coding region of mouse DHFR gene. **(B)** Representative genotyping results from tg-EC-DHFR and WT littermates. NC: water used for PCR as negative control. **(C)** Western blots showing increased expression of DHFR in aortas from tg-EC-DHFR mice in F1 generation.

2.3. Animal experiments and protocols

Diabetes was induced in WT and tg-EC-DHFR animals at the age of eight weeks old with two injections of STZ (100 mg/kg, i.v., #S0130, MilliporeSigma, Burlington, MA) as we previously published [1–3,26]. Animals were starved overnight by the end of 7 days. The next morning, blood glucose was measured with a OneTouch Ultra blood glucose meter (LifeScan, Milpitas, CA), and mice with blood glucose levels above 200 mg/dL were considered diabetic. Upon harvest, body weight, aortic superoxide production, aortic eNOS uncoupling activity, aortic nitric oxide bioavailability, and endothelium-dependent vasorelaxation were assessed.

In parallel experiments, eight-week-old apoE $^{-/-}$ mice were fed with high-fat diet (HFD) (caloric composition: 15.2% protein, 42% fat, 42.7% carbohydrates; #TD.88137, Envigo, Indianapolis, IN) for 16 weeks. To induce diabetic condition, mice were injected with STZ (100 mg/kg, i.p., #S0130, MilliporeSigma, Burlington, MA) on the 14th and 28th day after HFD feeding was started. Body weight and blood glucose levels were measured weekly. Animals were harvested for aortic eNOS uncoupling activity and atherosclerotic lesion formation at 24 weeks.

Littermates of apoE $^{-/-}$ and apoE $^{-/-}$ /tg-EC-DHFR mice at eightweek-old were fed with chow diet (caloric composition: 24.5% protein, 13.1% fat, 62.3% carbohydrates; PicoLab Rodent Diet 20, #5053, LabDiet, St. Louis, MO) or HFD (#TD.88137, Envigo, Indianapolis, IN) for 16 weeks. A subgroup of HFD-fed animals received two injections of STZ following the same protocol as in apoE $^{-/-}$ mice. Body weight was measured weekly. Blood glucose levels were measured at 16 weeks after overnight fasting as described above. Plasma samples were collected for determination of plasma lipids levels; and aortic atherosclerotic lesion

formation was assessed by Oil Red staining on the day of harvest.

Eight-week-old littermates of apoE^{-/-}/NOX1^{+/y} and apoE^{-/-}/NOX1^{-/y} were fed with HFD (#TD.88137, Envigo, Indianapolis, IN) or in-house customized HFD containing folic acid (15 mg/kg/day, FA, #F7876, MilliporeSigma, Burlington, MA) for 16 weeks. We have previously established protocols of oral FA administration as effective strategy to recouple eNOS in vivo [13,14,20,21,23]. STZ injection was carried out following the same protocol as in apoE^{-/-} mice. Body weight was measured weekly. Animals were harvested at the age of 24 weeks (after 16 weeks treatment) for assessment of atherosclerotic lesions in the isolated aortas.

2.4. Western blotting

Littermates of WT and tg-EC-DHFR mice were euthanized with CO_2 on the day of harvest. Tissue samples of aortas were collected and snapfrozen in liquid nitrogen after being cleaned of connective tissue and fat. Tissues were homogenized in ice-cold lysis buffer (20 mmol/L Tris-HCl pH 7.4, 150 mmol/L NaCl, 1 mmol/L EDTA, 1 mmol/L EGTA, 2.5 mmol/L sodium pyrophosphate, 1 mmol/L β -glycerophosphate, 1 mmol/L sodium orthovanadate, 1% Triton X-100) supplemented with protease inhibitor cocktail (1:100, #P8340, MilliporeSigma, Burlington, MA) before incubation on ice for 20 min. Then the supernatant was separated by centrifugation at 12,000 rpm for 10 min at 4°C. The supernatant was transferred to a new tube and the protein concentration was determined by a DC protein assay kit (#5000112, Bio-Rad, Hercules, CA). The protein lysates were loaded into 10% SDS-PAGE and transferred to nitrocellulose membranes. Proteins were probed with primary antibody for DHFR (1:1000, #H00001719-M01, Abnova, Taiwan), eNOS (1:1000,

#610297, BD Biosciences, Franklin Lakes, NJ) or β -actin (1:5000, #A2066, MiliporeSigma, Burlington, MA). The intensities of protein bands were analyzed and quantified by the NIH Image J software.

2.5. Isolation of aortic endothelial cells

Aortic endothelial cells (ECs) were isolated and subjected to Western blotting analysis as we published previously [10,12-15,21,27,28]. Briefly, freshly isolated aortas were cleaned of connective tissues and fat. Then aortas were cut into 2 mm rings and incubated with collagenase II (0.6 mg/mL, #17101015, Thermo Fisher Scientific, Waltham, MA) for 20 min at 37°C with gentle agitation. The endothelial cell (EC)-denuded rings were collected by forceps into a new tube. The endothelial cells disassociated were collected by centrifugation at 1,000 g for 3 min. Protein lysates were prepared from EC-denuded rings and EC fractions as described above. Approximately 20–30 μg proteins were loaded into 10% SDS-PAGE for Western blotting analysis as described above. Primary antibodies used for Western blotting were: DHFR (1:1000, #H00001719-M01, Abnova, Taiwan), eNOS (1:1000, #610297, BD Biosciences, Franklin Lakes, NJ) or β-actin (1:5000, #A2066, MiliporeSigma, Burlington, MA). NIH Image J software was used to quantify the intensity of the protein bands.

2.6. Isolation of mouse primary coronary endothelial cells

WT and tg-EC-DHFR animals (9.5-10.5 weeks) were used for isolation of primary coronary endothelial cells as previously described [29]. Animals were euthanized and whole hearts were collected. After perfusion with Hank's 1x Balanced Salt Solutions (HBSS, #SH30268.01, HyClone, Cytiva, Marlborough, MA) with 10 mmol/L HEPES, hearts were minced with dissecting scissors and incubated with collagenase type II (1 mg/mL, #17101015, Gibco, Thermo Fisher Scientific, Waltham, MA) and neutral protease (0.6 U/mL, #LS02109, Worthington Biochemical Corp., Lakewood, NJ) at 37°C for 75 min with occasional pipetting every 15 min. After incubation, digestion solution was filtered through sterile 40 µm cell strainer (#352340, Corning, Corning, NY) and cell pellet was collected by centrifugation at 400 g for 10 min. The cell pellets were washed 4 times with media M199 containing 2% iron-fortified calf serum (IFCS, #SH30072.04, HyClone, Cytiva, Marlborough, MA). Next, digestion solution was incubated with magnetic beads (#11-035, Thermo Fisher Scientific, Waltham, MA) conjugated with purified rat anti-mouse CD31 antibody (#550274, BD Biosciences, Franklin Lakes, NJ) on a shaker at 4°C for 60 min. The beads were washed with HBSS for 3 times if samples were to be used for HPLC (Shimadzu America Inc, Carlsbad, CA) determination of H₄B levels. Alternatively, the beads were washed 5 times with media M199 containing 2% IFCS and dissociated from cells by 20% fetal bovine serum (FBS) in media M199. Then the dissociated endothelial cells were seeded on cover slips in media M199 with 20% FBS for immunofluorescent staining to confirm the isolation of endothelial cells.

2.7. Immunofluorescent staining

Primarily isolated mouse coronary endothelial cells were cultured on cover slips. The staining and imaging processes were carried out as previously described [30]. Briefly, cells were fixed in 4% formaldehyde for 10 min at room temperature. Then the cells were washed with PBS and incubated with 0.1% Triton X-100 for 10 min. After 3 washes with PBS, the cells were blocked with PBS containing 3% BSA at room temperature for 1 h, followed by incubation with primary antibody of rat anti-mouse CD31 (1:100, #550274, BD Biosciences, Franklin Lakes, NJ) at 4°C overnight. The next morning, the cells were washed and incubated with donkey anti-rat IgG secondary antibody Alexa Fluor 488 (1:250, #A21208, Thermo Fisher Scientific, Waltham, MA) for 2 h at room temperature. The cover slides were mounted with Prolong Gold Antifade Mountant with DAPI (#P36935, Thermo Fisher Scientific,

Waltham, MA) after 3 washes and were kept in dark till imaged by a Nikon A1R Confocal Microscope (Nikon Corporation, Japan).

2.8. Determination of H₄B bioavailability using HPLC

H₄B levels from plasma samples and primarily isolated aortic and cardiac endothelial cells were determined using HPLC (Shimadzu America Inc, Carlsbad, CA) as we previously published [1,3,5,7,9,10, 12-14,20-23,27,28]. Freshly isolated plasma and aortic or coronary endothelial cells (conjugated to beads) were incubated with H₄B lysis buffer (0.1 mol/L phosphoric acid, 1 mmol/L EDTA, 10 mmol/L DL-dithiothreitol) on ice for 20 min. Lysates were collected by centrifugation at 12,000 rpm for 5 min at 4°C. Then, samples were subjected to differential oxidation under acidic condition (0.2 mol/L trichloroacetic acid with 2.5% $\rm I_2$ and 10% KI) or alkalytic condition (0.1 mol/L NaOH with 0.9% I_2 and 1.5% KI). After centrifugation, 35 μL of the supernatant was injected into the HPLC system for analysis by a fluorescent detector. Excitation and emission wavelengths of 350 nm and 450 nm were used to detect H₄B and its oxidized species. The H₄B levels were calculated according to a standard curve of H₄B (#T4425, MilliporeSigma, Burlington, MA) generated following the same protocol.

2.9. Determination of eNOS uncoupling activity and total superoxide production by Electron spin resonance (ESR)

Freshly isolated aortas were carefully and thoroughly cleaned of connecting tissues and fat. Aortic tissues were homogenized in lysis buffer containing 1:100 protease inhibitor cocktail as mentioned above. Protein concentrations of the tissue lysates were determined with the same method as described in the Western blotting section above. Superoxide-specific spin trap methoxycarbonyl-2,2,5,5-tetramethylpyrrolidine (CMH, 500 µmol/L, #ALX-430-117-M250, Enzo Life Sciences, Farmingdale, NY) was prepared in nitrogen gas bubbled modified Krebs/HEPES buffer (KHB) (99 mmol/L NaCl, 4.69 mmol/L KCl, 1.03 mmol/L KH₂PO₄, 2.50 mmol/L CaCl₂, 1.20 mmol/L MgSO₄, 25.0 mmol/ L NaHCO₃, 5.6 mmol/L glucose, and 20.0 mmol/L Na-HEPES, pH 7.35) containing diethyldithiocarbamic acid (5 µmol/L, D3506, MilliporeSigma, Burlington, MA) and deferoxamine (25 µmol/L, D9533, MilliporeSigma, Burlington, MA). Tissue lysates were mixed with freshly prepared spin traps and loaded into glass capillaries for analysis of superoxide signal using the ESR spectrometer (eScan, Bruker, Billerica, MA) as we previously published. Three measurements of superoxide production were carried out for each sample in the presence of water (as baseline), L-NAME (a NOS inhibitor, 10 μM, #80587, Cayman Chemical, Ann Arbor, MI), or SOD (20 U/mL, #ALX-202-022-UT50, Enzo Life Sciences, Farmingdale, NY). The eNOS uncoupling activity is shown as superoxide production with or without L-NAME after normalization by protein concentration. It is known that uncoupled eNOS produces superoxide. L-NAME treatment leads to reduced superoxide signal when eNOS is uncoupled. L-NAME treatment leads to increased superoxide signal when eNOS is coupled or re-coupled, due to lack of buffering effects of NO on scavenging superoxide. The ESR settings used were as follows: center field 3,479, sweep width 9 G, microwave frequency 9.79 GHz, microwave power 21.02 mW, modulation amplitude 2.47 G, points of resolution 512, and receiver gain 1000.

2.10. Determination of aortic nitric oxide bioavailability by ESR

Aortic NO bioavailability was determined by ESR as we previously described [1,7,9,10,12,18,21–23,28,30,31]. Freshly isolated aortas were cut into 2 mm rings and then incubated with NO-specific spin trap ${\rm Fe}^{2+}({\rm DETC})_2$ (0.5 mmol/L) colloid at 37°C for 1 h in the presence of calcium ionophore A23187 (10 μ mol/L, #C7522, MilliporeSigma, Burlington, MA). After the incubation, the aortic rings were snap-frozen in liquid nitrogen and loaded into ESR spectrometer (eScan, Bruker, Billerica, MA) in a figure Dewar. The ESR settings used were as follows:

center field, 3,440, sweep width, 100 G, microwave frequency, 9.79 GHz, microwave power 13.26 mW, modulation amplitude, 9.82 G, points of resolution 512, and receiver gain 356.

2.11. Assessment of vasorelaxation using myograph

Freshly isolated aortic rings were cut into 2 mm rings and vasorelaxation was examined using Myograph (620 M, Danish Myo Technology, Denmark) as we previously published [1-3,5,7,12,18]. In brief, the aortic rings were mounted on the parallel pins in a chamber of Myograph and equilibrated at 37°C for 30 min in 95% oxygen/5% carbon dioxide-bubbled PSS Bicarbonate buffer (130 mmol/L NaCl, 4.7 mmol/L KCl, 1.18 mmol/L KH₂PO₄, 1.17 mmol/L MgSO₄, 14.9 mmol/LNaHCO₃, 5.5 mmol/L glucose, 0.026 mmol/L EDTA, 1.6 mmol/L CaCl₂). The aortic rings were pre-stretched with a tension of 12 mN and high potassium PSS Bicarbonate buffer (74.7 mmol/L NaCl, 60 mmol/L KCl, 1.18 mmol/L KH₂PO₄, 1.17 mmol/L MgSO₄, 14.9 mmol/l NaHCO₃, 5.5 mmol/L glucose, 0.026 mmol/L EDTA, 1.6 mmol/L CaCl₂). The vasorelaxation in response to incremental concentrations of acetylcholine $(10^{-9} \text{ to } 10^{-6} \text{ mol/L})$ in the presence of phenylephrine (1 µmol/L, #P6126, MilliporeSigma, Burlington, MA) was recorded. Similarly, second-order branches of mesenteric artery were isolated and mounted to Myograph. Different from aortic rings, a tension of 3 mN was used for pre-stretch for mesenteric arteries. And the tension in response to acetylcholine (10⁻⁹ to 10⁻⁶ mol/L, #A2661, MilliporeSigma, Burlington, MA) in the presence of norepinephrine (3 µmol/L, #A9512, MilliporeSigma, Burlington, MA) was recorded. Data acquisition was performed by Data-Trax hardware and Lab-Trax software (World Precision Instruments, Sarasota, FL).

2.12. Oil red O (ORO) staining of atherosclerotic lesions

A stock of 0.5% (w/v) of ORO (#O0625, MilliporeSigma, Burlington, MA) was prepared in isopropanol. The working solution of 0.3% Oil Red O was prepared by diluting the stock solution with deionized water and filtration with 0.2 μ m filter. Cleaned mouse aortas were rinsed in PBS containing 0.5% Triton X-100 and stained with ORO working solution for 30 min at room temperature. Then the aortas were destained with isopropanol and washed in distilled water for 20 min. Images were captured using Leica Microscope M60 with Leica Microsystems Digital Camera EC3. Lesion areas and areas of whole aortas were analyzed by NIH Image J Software. The percentage of lesion areas was calculated as 100% lesion area/area of whole aorta.

2.13. Determination of plasma total cholesterol, high-density lipoprotein cholesterol (HDL), low-density lipoprotein cholesterol (LDL)

Plasma was isolated by centrifugation of fresh blood at 2,000 rpm for 20 min at 4°C. Plasma levels of total cholesterol were measured using Cholesterol Reagent Set (#C7510-120, Pointe Scientific, Canton, MI), and calculated according to the cholesterol standard (#C3045, MilliporeSigma, Burlington, MA). Plasma levels of LDL cholesterol were measured using LDL Cholesterol Reagent Set (#L7574-40, Pointe Scientific, Canton, MI) and calculated according to the LDL cholesterol standard (#H7545-CAL, Pointe Scientific, Canton, MI). For HDL measurement, plasma samples were mixed with equal volume of HDL Cholesterol Reagent Set (#7511-60, Pointe Scientific, Canton, MI), and precipitation was separated by centrifugation at 2000 g for 10 min. Then plasma levels of HDL were measured from the supernatant also using the Cholesterol Reagent Set and calculated according to the HDL Standard (#H7512-STD, Pointe Scientific, Canton, MI).

2.14. Statistical analysis

All data are presented as Mean \pm SEM. Student's t-test was used to compare the difference between two groups. One-way ANOVA was used

for comparison between multiple groups with Newman-Keuls post-hoc test. Data of vasorelaxation and body weight were analyzed by two-way ANOVA, Bonferroni post-hoc was used after two-way ANOVA analyses. The p value < 0.05 was considered significant.

3. Results

3.1. Generation of endothelial-specific DHFR transgenic mice

Endothelial-specific DHFR transgenic mice were generated by microinjection of a DNA fragment containing endothelial-specific Ve-Cadherin promoter followed by the coding region of mouse DHFR gene (NM_010049) (Fig. 1A). Detailed information of transgenic construct generation and design of genotyping primers are presented in the Methods section above. Genotyping results (Fig. 1B) showed successful generation of tg-EC-DHFR mice and the two pairs of genotyping primers provide consistent results of genotyping. As shown in Fig. 1C, Western blotting analyses indicate that tg-EC-DHFR mice had stable endothelial specific overexpression of DHFR in aortic tissues when compared with wild type (WT) littermates.

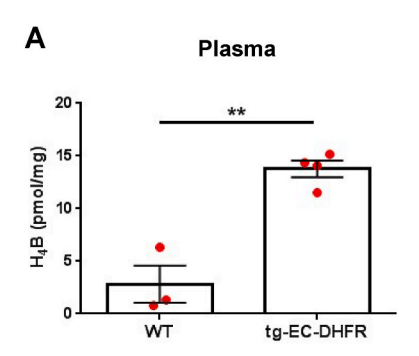
Next, we examined whether increased endothelial DHFR expression resulted in increased H₄B bioavailability in the tg-EC-DHFR mice. As shown in Fig. 2A, tg-EC-DHFR mice displayed significantly increased plasma H₄B levels compared to WT littermates. Of note, the H₄B bioavailability was also markedly increased in endothelial cells primarily isolated from coronary artery (Fig. 2B, Suppl. Fig. 4). Collectively, these data clearly demonstrate that the successfully generated tg-EC-DHFR mice have overexpressed DHFR protein that is functionally more active in maintaining higher levels of H₄B bioavailability.

3.2. Endothelial-specific DHFR transgenesis recoupled eNOS in diabetes

We have previously shown that DHFR expression was diminished while eNOS was uncoupled in STZ-induced diabetic mice [1,3]. To study whether endothelial overexpression of DHFR recouples eNOS, we induced diabetes by STZ injection in both WT and tg-EC-DHFR mice as previously published [1–3,26]. In accordance with previous reports, STZ injection resulted in reduced body weight and elevated fasting glucose levels (Fig. 3A–B). Body weight loss after STZ injection was similar in both WT littermates and tg-EC-DHFR mice (Fig. 3A), while the elevation in fasting blood glucose levels was also similar in tg-EC-DHFR mice and WT littermates (Fig. 3B). Of note, animals from a separate founder #73-7 showed similar results (Suppl. Fig. 2).

Next, we examined aortic total superoxide production and eNOS uncoupling activity using ESR in aortas of STZ-treated WT and tg-EC-DHFR mice. Consistent to our previous findings [1,3], STZ injection induced a substantial increase in total superoxide production in WT diabetic mice (Fig. 4A). While no difference in total superoxide production was observed at baseline between WT and tg-EC-DHFR mice, tg-EC-DHFR mice had no increase in superoxide production in response to STZ induction of diabetes (Fig. 4A). Furthermore, eNOS was uncoupled in STZ-induced diabetic mice as we published previously, which was abolished in tg-EC-DHFR mice made diabetic (Fig. 4B). Of note, uncoupled eNOS, characterized by decreased superoxide production in the presence of NOS inhibitor L-NAME, produces superoxide instead of NO. Alongside uncoupling of eNOS, aortic NO bioavailability was significantly and expectedly decreased in WT diabetic mice, which was completely restored in tg-EC-DHFR mice made diabetic (Fig. 4C-D). These data clearly indicate that eNOS uncoupling activity in diabetes can be completely attenuated by endothelial-specific DHFR overexpression to result in recoupling of eNOS to improve NO bioavailability.

В



Primarily isolated coronary ECs

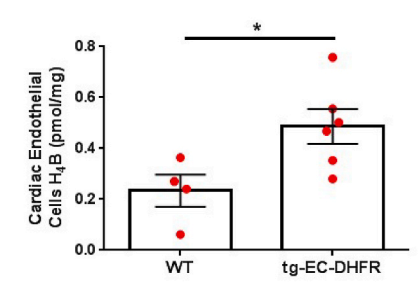
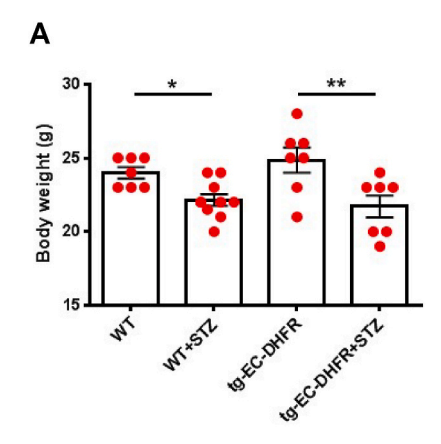


Fig. 2. Elevated endothelial cell and circulating levels of H_4B in tg-EC-DHFR mice. Circulating and endothelial cell H_4B levels were determined using HPLC as we previously published. Data indicate H_4B levels in plasma (A) and primarily isolated coronary endothelial cells (B) were markedly elevated in tg-EC-DHFR transgenic mice comparing to WT mice. *p < 0.05, **p < 0.01. n = 3-4 for (A), n = 4-6 for (B).



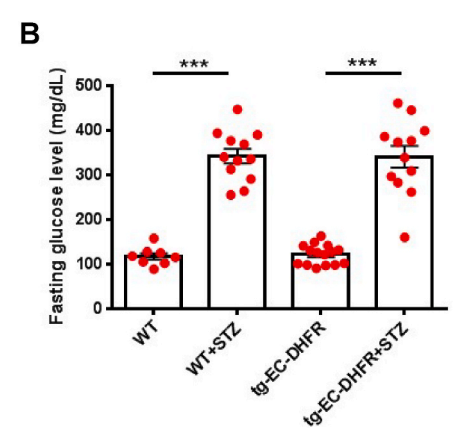


Fig. 3. Endothelial-specific DHFR transgenesis had no effects on body weight and fasting glucose levels in response to STZ induction of diabetes. WT and tg-EC-DHFR mice were induced of diabetes using STZ as we previously published. (A) Body weight in WT and tg-EC-DHFR mice with or without STZ treatment. *p < 0.05, **p < 0.01. n = 7, 9, 7 and 7. (B) Fasting glucose levels in WT and tg-EC-DHFR mice with or without STZ treatment. ***p < 0.001. n = 8, 12, 15 and 12.

3.3. Endothelial-specific DHFR transgenesis restored vasorelaxation in diabetes

Endothelium-dependent vasorelaxation is impaired in type 1 diabetes mellitus. We have previously shown that vasorelaxation of freshly isolated aortic rings is defective in STZ-induced diabetic mice [1,3]. To examine whether recoupling of eNOS and restoration in NO bioavailability in tg-EC-DHFR mice made diabetic are accompanied by improved vasorelaxation, we examined endothelium-dependent vasorelaxation of aortas and mesenteric arteries isolated from STZ-injected WT and tg-EC-DHFR mice. We found that endothelial-specific DHFR transgenesis completely preserved endothelium-dependent vasorelaxation in response to acetylcholine in aortic rings (Fig. 5A). Moreover, we isolated second order mesenteric arteries from WT and tg-EC-DHFR mice with or without STZ treatment. Similar to responses in aortas, endothelial-specific DHFR transgenesis also completely preserved endothelium-dependent vasorelaxation in mesenteric arteries (Fig. 5B).

3.4. Endothelial-specific DHFR transgenesis attenuated diabetic atherogenesis in STZ-injected apo ${\rm E}^{-/-}$ mice

We next examined the hypothesis that restoration of eNOS function and improvement in endothelial-dependent vasorelaxation/endothelial function in tg-EC-DHFR mice are functionally effective in attenuating diabetic atherogenesis. To address this, we developed a protocol of inducing diabetic atherosclerosis by injecting STZ twice into high-fat diet (HFD) fed apoE^{-/-} mice (Fig. 6A). Blood glucose levels were increased by STZ injection (Fig. 6B), suggesting successful induction of diabetes by STZ in apoE^{-/-} mice. Significant body weight loss was

observed in HFD-fed apo $E^{-/-}$ mice treated with two STZ injections (Fig. 6C). More importantly, STZ injection induced accelerated atherosclerotic lesion formation in HFD-fed apo $E^{-/-}$ mice, as assessed by oil red staining (Fig. 6D and E).

To test our hypothesis of a protective role of endothelial-specific transgenesis on diabetic atherogenesis, we crossed tg-EC-DHFR mice with apoE $^{-/-}$ mice to generate apoE $^{-/-}$ /tg-EC-DHFR mice (details see Methods section). The apoE $^{-/-}$ and apoE $^{-/-}$ /tg-EC-DHFR mice of 8 weeks old were treated with chow diet, HFD, or HFD + STZ till the mice were 6 months old. As shown in Fig. 7A and B, formation of atherosclerotic lesion was significantly increased in apoE $^{-/-}$ mice treated with HFD + STZ, compared to apoE $^{-/-}$ mice on HFD alone, indicating accelerated atherosclerosis under diabetic environment. This further increase in atherosclerotic lesion formation was completely blunted in apoE $^{-/-}$ /tg-EC-DHFR mice treated with HFD + STZ, indicating that endothelial-specific DHFR transgenesis is robustly effective in attenuating accelerated diabetic atherogenesis.

Metabolic features of the mice were also compared. The body weight was not different between HFD fed apoE $^{-/-}$ and apoE $^{-/-}$ /tg-EC-DHFR mice treated with HFD + STZ (Fig. 7C). Furthermore, we measured fasting glucose levels and plasma lipid levels in different groups. Intriguingly, fasting glucose was normalized by endothelial DHFR overexpression in HFD and STZ-treated apoE $^{-/-}$ mice (Fig. 7D), which warrants further investigation. Plasma total cholesterol and LDL levels were increased by treatment of HFD and HFD + STZ in apoE $^{-/-}$ mice, but the increases were not affected by endothelial-specific DHFR transgenesis (Fig. 7E–F). Similarly, plasma HDL levels were not affected by endothelial-specific DHFR transgenesis, although HFD and HFD + STZ attenuated HDL levels in apoE $^{-/-}$ mice (Fig. 7G). These data suggest

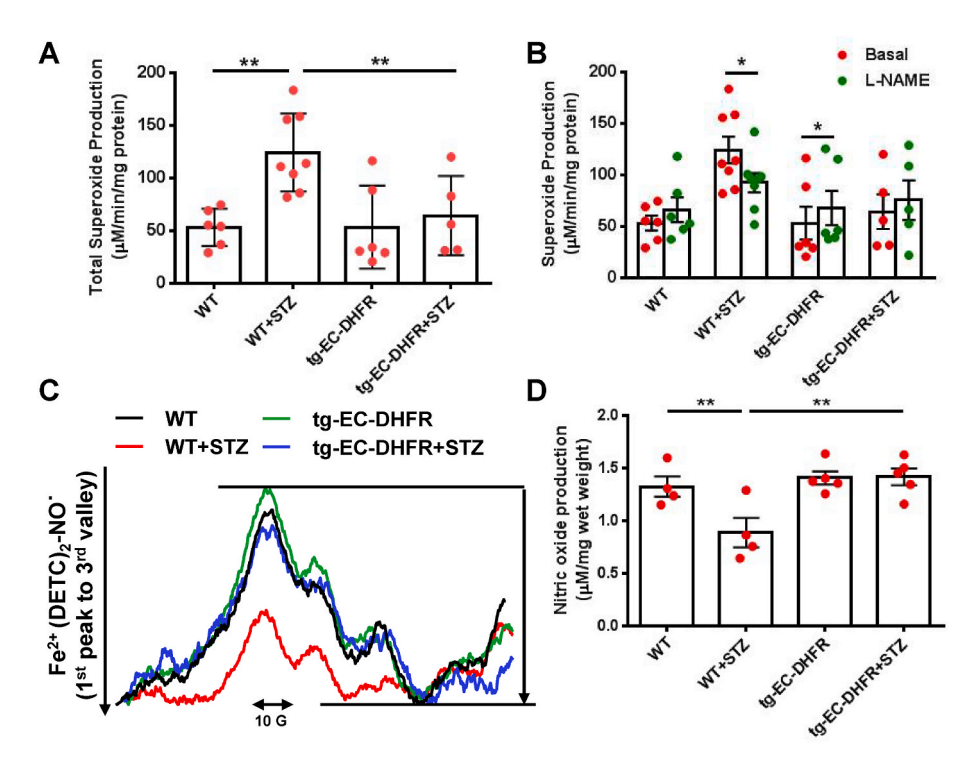


Fig. 4. Endothelial-specific DHFR transgenesis recoupled eNOS and improved nitric oxide bioavailability in STZ-induced diabetic mice. WT and tg-EC-DHFR mice were induced of diabetes using STZ as we previously published. (A) Increased aortic superoxide production in diabetes was completely attenuated by endothelial specific DHFR transgenesis. **p < 0.01. n = 6, 8, 6 and 5. (B) eNOS uncoupling activity in diabetes, reflected by μ -NAME-inhibitable superoxide production, was completely alleviated by endothelial specific DHFR transgenesis. *p < 0.05. n = 6, 8, 6 and 5. (C, D) Representative and quantitative data of aortic NO bioavailability indicating impaired NO bioavailability in diabetes was fully restored by endothelial specific DHFR transgenesis. *p < 0.01. n = 4, 4, 5 and 5.

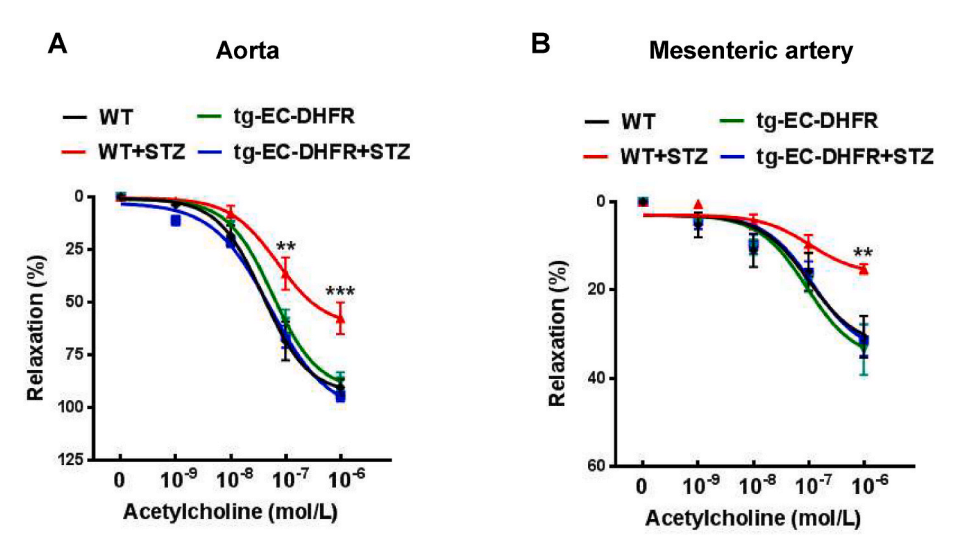


Fig. 5. Endothelial-specific DHFR transgenesis improved vasorelaxation in STZ-induced diabetic mice. WT and tg-EC-DHFR mice were induced of diabetes using STZ as we previously published. Aortas and mesenteric arteries were freshly isolated and subjected to analysis of vasodilatiaon using myograph as we previously describe. Data indicate that impaired endothelium-dependent vasorelaxation in response to acetylcholine in pre-contracted aorta (A) or mesenteric artery (B) of diabetic mice was completely restored by endothelial-specific DHFR transgenesis. **p < 0.01, ***p < 0.001 compared to WT or tg-EC-DHFR + STZ. n = 5, 4, 9 and 7 for (A) and n = 5 for (B).

that endothelial-specific overexpression of DHFR does not directly impact on lipid metabolism.

3.5. NOX1 deletion or FA recoupling of eNOS attenuated diabetic acceleration of atherogenesis in apo $E^{-/-}$ mice

As we have previously shown, NOX1 is specifically involved in upstream activation of eNOS uncoupling in STZ-induced diabetes [3]. To

examine whether knockout of NOX1 is protective of diabetic atherogenesis via alleviation of eNOS uncoupling activity, we generated apoE $^{-/-}$ and NOX1 $^{-/y}$ double knockout mice. Littermates with wild type NOX1 gene (apoE $^{-/-}$ /NOX1 $^{+/y}$ mice) were used as experimental control. Importantly, we found that NOX1 deletion markedly reduced atherosclerotic lesion formation in HFD + STZ-treated apoE $^{-/-}$ /NOX1 $^{+/y}$ mice (Fig. 8). Oral administration of FA, known to upregulate DHFR expression in vivo by our previous studies [3,6,10,13,

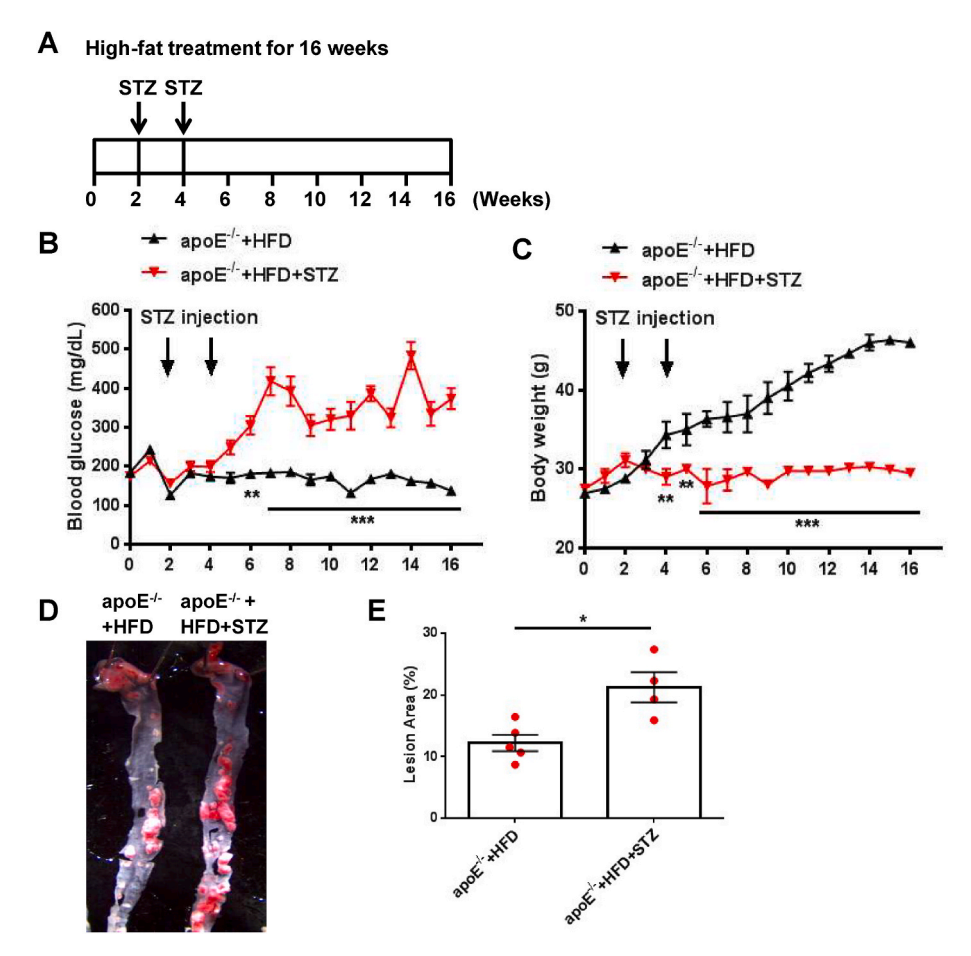


Fig. 6. Induction of diabetic atherogenesis in apo $E^{-/-}$ mice by HFD and STZ treatment. (A) A schematic protocol of induction of diabetic atherogenesis in apo $E^{-/-}$ mice. Male apo $E^{-/-}$ mice were fed high-fat diet (HFD) for 16 weeks while receiving STZ injection twice at week 2 and week 4. (B) Fasting blood glucose levels were increased in STZ treated apo $E^{-/-}$ mice. **p < 0.01, ***p < 0.001. n = 3-4. (C) Body weight was reduced in STZ treated apo $E^{-/-}$ mice. **p < 0.01, ***p < 0.001. n = 6-8. (D, E) Representative images and quantitative data of Oil Red O staining assessment of atherosclerotic lesion formation, indicating markedly increased atherogenesis in apo $E^{-/-}$ HFD + STZ compared to apo $E^{-/-}$ + HFD mice.

14,20–22], also attenuated atherosclerotic lesion formation in HFD + STZ-treated apoE $^{-/-}$ /NOX1 $^{+/y}$ mice (Fig. 8). Interestingly, administration of FA failed to further restrain lesion formation in HFD + STZ-treated apoE $^{-/-}$ /NOX1 $^{-/y}$ mice (Fig. 8), indicating that FA/DHFR and NOX1/DHFR/eNOS uncoupling axis shares the similar target of modulation in DHFR function in attenuating/triggering diabetic atherogenesis.

4. Discussion

In this study, we generated endothelial-specific DHFR transgenic mice and found that endothelial-specific DHFR transgenesis recoupled eNOS to abrogates STZ-induced endothelial dysfunction and to attenuate accelerated diabetic atherogenesis in HFD/STZ-treated apoE^{-/-} mice. The most significant finding of this study is the first demonstration that endothelial-specific/targeted DHFR overexpression effectively alleviates endothelial dysfunction and formation of atherosclerotic lesions. In addition, we found that NOX1 lies upstream of eNOS uncoupling in accelerating diabetic atherogenesis, deletion of which completely blocked STZ-induced progression of diabetic atherosclerosis in apoE^{-/-} mice. Furthermore, oral FA administration to preserve DHFR function was also robustly effective in alleviating diabetic atherogenesis. These findings establish a central role of endothelial DHFR deficiency in mediating endothelial dysfunction and accelerated atherogenesis in diabetes via the mechanism of eNOS uncoupling, targeting of which with endothelial-specific transgenesis, NOX1 deletion or oral FA administration is completely effective in reversing these phenotypes of vascular complications in diabetes (Fig. 9).

Patients with diabetes primarily die of cardiovascular complications. In particular, atherosclerosis is known to contribute to more than 80% of the cardiovascular disease-associated mortality and disability [32]. Despite of accumulated evidence on close correlation between diabetes and accelerated atherogenesis, the mechanisms by which diabetes exaggerate atherogenesis remain incompletely understood. Others and we have recently demonstrated a central role of eNOS uncoupling in diabetic endothelial dysfunction [1,3,5,9-12,16,17], which is also supported by the findings in this study. In the present study, we demonstrated that increased eNOS uncoupling activity and lesion formation in STZ-injected apo $E^{-/-}$ mice fed with HFD, when compared with non-STZ injected mice (Fig. 6D-F), indicating potential role of eNOS uncoupling in accelerated atherosclerosis in diabetes. Furthermore, recoupling of eNOS by oral folic acid administration (Fig. 8) or endothelial specific DHFR overexpression (Fig. 7A-B), completely alleviated enhanced lesion formation induced by STZ, clearly demonstrating a causal role of eNOS uncoupling in diabetic atherogenesis.

The most intriguing and innovative finding of this study is identification of an important and critical role of endothelial DHFR in the maintenance of vascular function in T1DM to protect against diabetic atherogenesis. eNOS uncoupling occurs consequent to oxidative inactivation of its cofactor H_4B . It has been reported that daily oral H_4B supplementation reduces atherosclerotic lesion formation in apo $E^{-/-}$ mice [33,34], although this might not be translatable to clinical practice

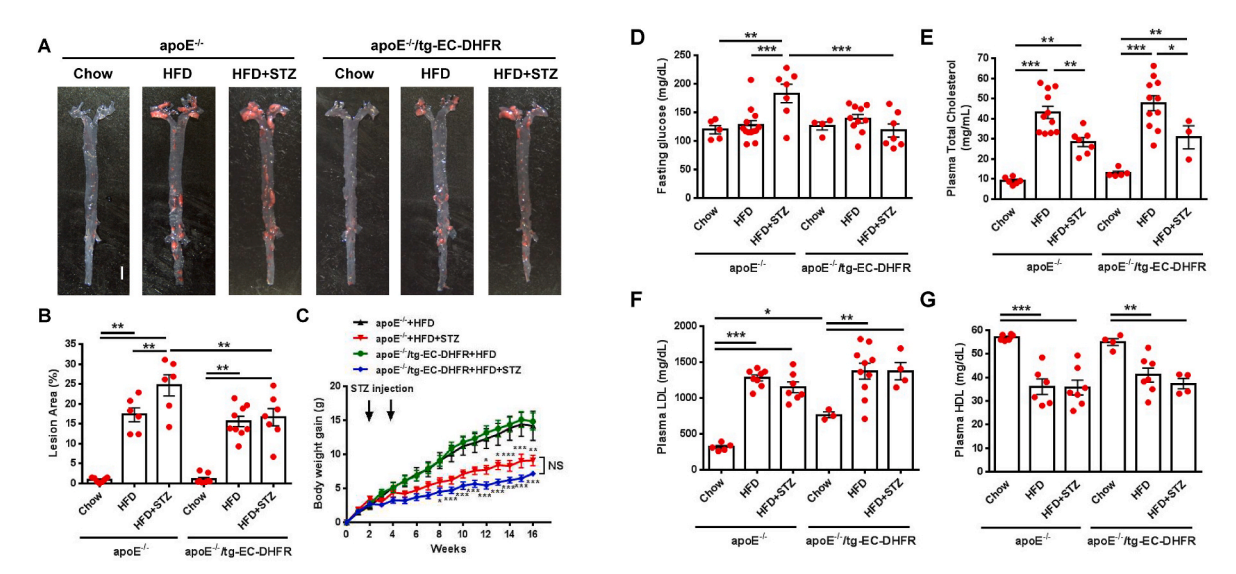


Fig. 7. Endothelial-specific DHFR transgenesis abrogated diabetic atherogenesis in apoE $^{-/-}$ mice. Male apoE $^{-/-}$ mice were fed high-fat diet (HFD) for 16 weeks while receiving STZ injection twice at week 2 and week 4 to induce diabetic atherogenesis. (**A, B**) Representative images and quantitative data of Oil Red O stained aortas from all experimental groups, indicating abrogation of atherogenesis under control and diabetic environment by endothelial DHFR transgenesis in HFD and HFD + STZ-treated apoE $^{-/-}$ mice. **p < 0.01. n = 7, 6, 6, 8, 9, and 7. (**C**) Body weight gain was not changed by endothelial DHFR transgene in HFD or HFD + STZ-treated apoE $^{-/-}$ mice. *p < 0.05, **p < 0.01, ***p < 0.001 vs. group of the same genotype with HFD treatment. NS: not significant. n = 7. (**D**) Fasting glucose levels in all experimental groups, indicating attenuation of elevated blood glucose in diabetic environment by endothelial-specific DHFR transgenesis. **p < 0.01, ***p < 0.001. n = 5, 13, 7, 4, 10, 7. Plasma triglycerides (**E**), total cholesterol (**F**), LDL (**G**), and HDL (**H**) levels in all experimental groups, indicating no effects on circulating lipid profiles of endothelial-specific DHFR transgenesis. *p < 0.05, **p < 0.01, ***p < 0.001. n = 5, 11, 7, 2, 12, 4 for (**E**). n = 6, 11, 7, 5, 11, 3 for (**F**). n = 5, 8, 7, 3, 10, 4 for (**G**). n = 6, 6, 7, 4, 7, 4 for (**H**).

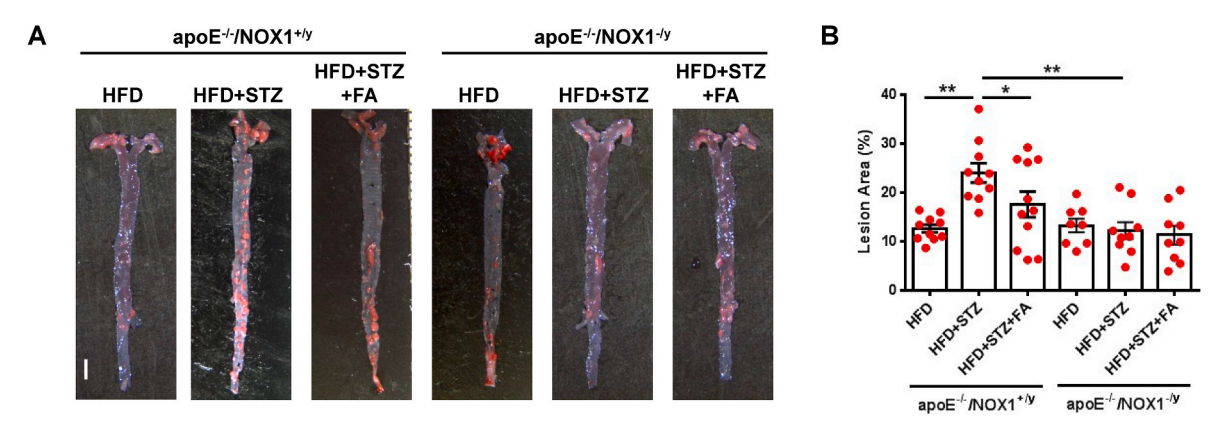


Fig. 8. NOX1 deletion or oral folic acid administration alleviated diabetic atherogenesis in apo $E^{-/-}$ mice. Double knockout mice of apo $E^{-/-}$ /NOX1^{+y} were generated in house and then subjected to high-fat diet feeding and STZ induction of diabetes. (A & B) Representative images and quantitative data of Oil Red stained aortas from all experimental groups, indicating attenuation of atherosclerosis by NOX1 knockout or oral FA administration. *p < 0.05, **p < 0.01. n = 10, 10, 11, 8, 9, 9. Scale bar: 2 mm.

due to instability of H_4B . H_4B is unstable and rapidly oxidizable, which limits its application [35]. Therefore, it is anticipated that modulation of H_4B metabolic enzymes to preserve H_4B bioavailability might be of better therapeutic applicability. Our previous studies have revealed endothelial-specific deficiency of DHFR alongside aortic eNOS uncoupling activity in mice with diabetes, hypertension, and aneurysm formation [1,3,9,10,12–15,21–23,28], establishing a critical role of endothelial DHFR function in the modulation of eNOS coupling activity to preserve endothelial integrity to protect against these pathological conditions. In the present study, we found that endothelial-specific DHFR transgenesis was indeed robustly effective in attenuating H_4B deficiency and eNOS uncoupling activity to result in abrogated endothelial dysfunction and diabetic atherogenesis. Our data for the first time innovatively implicate a cell type-specific strategy for the treatment of diabetic atherogenesis.

Our previous work has established that activation of NOXs induces

eNOS uncoupling through ROS-dependent H₄B deficiency, which prolongs oxidative stress to result in endothelial dysfunction. Many of the additional studies from us and others further indicate that the crosstalk between activation of NOX(s) and eNOS uncoupling may involve different NOX isoform(s) in different cardiovascular and metabolic diseases [6]. For example, NOX1/2/4-dependent eNOS uncoupling plays an important role in the formation of abdominal aortic aneurysm (AAA) in Ang II infused hph-1 mice made double knockout of NOX1, NOX2 or NOX4 [6,13,15,27]. More recently, we reported that NOX4-dependent activation of TGF-β pathway triggers eNOS uncoupling to induce thoracic aortic aneurysm (TAA) formation in the Marfan syndrome Fbn1 mice [21]. NOX2 and NOX4 have been implicated in ROS production to mediate pressure overload and Ang II-induced cardiac hypertrophy and heart failure [6,36-38]. Others and we have defined detailed mechanisms of NOX4 activation in triggering eNOS uncoupling during cardiac ischemia-reperfusion injury, resulting in excessive ROS production,

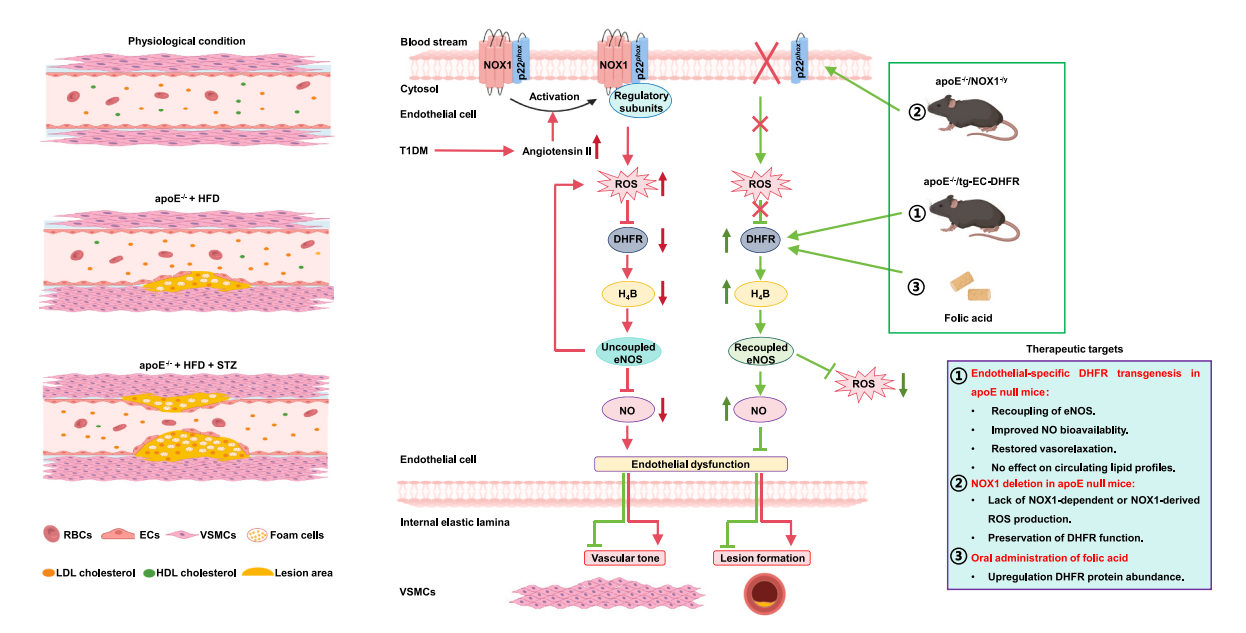


Fig. 9. Schematic illustration of therapeutic effects of endothelial-specific DHFR transgenesis, NOX1 deletion or oral administration of FA on diabetic endothelial dysfunction and accelerated atherogenesis.

myocyte apoptosis, necrosis and autophagy, and consequent development of infarct and loss in cardiac function [6,39–43]. Of note, we have clearly documented differential roles of BMP4-activation of NOX1 in mediating eNOS uncoupling and endothelial dysfunction in T2DM, whereas Ang II-activation of NOX1 induces eNOS uncoupling and dysfunction of endothelium in T1DM [3,5,7]. Therefore, understanding the specific NOX isoform(s) that is(are) involved under different pathological conditions may enable specific and accurate treatment strategies.

Studies from our group have shown that aortic expression of NOX1 is robustly up-regulated in STZ-induced diabetic mice by more than threefold, which is associated with increased ROS generation and endothelial dysfunction [1,3]. Likewise, increased NOX1 expression in aortas was also reported in STZ-induced diabetic rats, along with endothelial dysfunction and decrease in NO production [44]. Moreover, mice deficient in NOX1, or the NOX1 binding partner TLR2 innovatively defined by our recent studies, are protected from STZ-induced eNOS uncoupling and endothelial dysfunction in T1DM or high fat diet feeding induced eNOS and vascular dysfunction in T2DM respectively [3,7]. Therefore, our data consistently and reproducibly demonstrate that selective activation of NOX1, instead of NOX2 or NOX4, mediates diabetic uncoupling of eNOS and hence, development of vascular complications, implicating a potential role of NOX1 in diabetic acceleration of atherosclerosis. Indeed, in this present study, we found that NOX1 deletion markedly alleviated aortic lesion formation in HFD + STZ-treated apo $E^{-/-}$ mice (Fig. 8), indicating a unique and selective role of NOX1 in attenuating diabetic atherogenesis that is attributed to downstream mechanistic effector of uncoupled eNOS.

Our previous studies have demonstrated that FA upregulates protein abundance of DHFR to recouple eNOS in cultured endothelial cells [10]. Furthermore, oral intake of FA specifically restores endothelial DHFR to recouple eNOS and prevent aneurysm formation in various genetic mice infused with Ang II for AAA formation, or in Fbn^{Cl039G/+} Marfan syndrome mice as a classical model for the development of TAA [10,18,20, 21,23]. More importantly, oral administration of FA recouples eNOS to improve aortic vasodilatation in STZ-induced type 1 diabetic mice [45]. With uncoupled eNOS being the primary causal factor of endothelial dysfunction and diabetic atherogenesis as demonstrated by data in the present study and reported earlier, we hypothesize that FA recoupling of eNOS would also attenuate atherosclerotic lesion formation in HFD +

STZ-treated apoE $^{-/-}$ mice. Indeed, we found that FA treatment markedly decreased extents of atherosclerotic lesion in HFD + STZ-treated apoE $^{-/-}$ /NOX1 $^{+/y}$ mice (Fig. 8). Of note, FA had no additional effects in NOX1 deleted mice indicating NOX1/DHFR/eNOS uncoupling and FA/DHFR/eNOS recoupling shares the same target of endothelial DHFR for pathological progression and effective therapies. These data strongly elucidate clinical significance and applicability of FA in serving as a new treatment option for accelerated atherosclerosis in diabetes, and suggest that oral FA intake can be considered as an alternative strategy to endothelial-targeted DHFR gene threapy in the treatment of diabetic atherogenesis.

One interesting findings of this study is that fasting glucose levels were decreased by endothelial-specific DHFR transgenesis in HFD + STZ-treated apo $E^{-/-}$ mice (Fig. 7D). These findings seem to suggest a role of normal endothelial eNOS function in the modulation of glucose metabolism/homeostasis, which warrants further investigation. On the other hand, body weight gain was unchanged in apoE^{-/-}/tg-EC-DHFR + HFD + STZ mice when compared with apoE $^{-/-}$ + HFD + STZ mice upon endothelial specific overexpression of DHFR (Fig. 7C), indicating that fat metabolism may not be related to eNOS recoupling associated reduction in blood glucose levels. Likewise, the plasma levels of total cholesterol, LDL, and HDL were not altered by endothelial-specific DHFR transgenesis in HFD + STZ-treated apo $E^{-/-}$ mice (Fig. 7E-G), indicating that recoupling of eNOS and restoration of endothelial function may not directly link to lipid metabolism pathways. Though there are changes in insulin signaling in high-fat fed animals, no evidence is available as to whether insulin signaling directly impacts on DHFR expression and function. In future studies, it might be of significance to specifically manipulate insulin resistance to examine consequent responses in DHFR/eNOS axis to affect endothelial function and progression of diabetic atherosclerosis.

Taken together, our present study for the first time provides direct evidence of endothelial DHFR overexpression in restoring endothelial function to abrogate atherosclerotic lesion formation in diabetic animals through recoupling of eNOS. These compelling observations, coupled with our previous findings on an endogenous role of endothelial specific DHFR deficiency in the pathogenesis of vascular diseases including hypertension and aortic aneurysms, indicate that endothelial-specific targeting of DHFR can serve as a novel and robust therapeutic strategy for accelerated diabetic atherogenesis. In addition, we demonstrated a

critical intermediate role of NOX1-dependent eNOS uncoupling in diabetic atherogenesis, which can be corrected by NOX1 deletion, endothelial specific DHFR gene therapy or oral folic acid administration. Our results clearly demonstrate that regimes effective in endothelial specific activation of DHFR, such as via inhibition of NOX1, DHFR gene therapy and FA intake, might serve as novel and robust treatment options to alleviate endothelial dysfunction to prevent devastating and lethal atherosclerotic complications in patients with diabetes.

CRediT authorship contribution statement

Yixuan Zhang: Data curation, Formal analysis, Methodology, Writing – original draft. Ji Youn Youn: Data curation, Formal analysis. Kai Huang: Data curation. Yuhan Zhang: Data curation, Formal analysis. Hua Cai: Conceptualization, Formal analysis, Funding acquisition, Investigation, Methodology, Project administration, Supervision, Validation, Visualization, Writing – original draft, Writing – review & editing.

Declaration of competing interest

The authors declare that they have no conflicts of interest with the contents of this article.

Acknowledgement

This work was supported by the National Heart, Lung, and Blood Institute grants HL077440 (H. C.), HL088975 (H. C.), HL142951 (H. C.), HL154754 (H. C. and A. M.), HL162407 (H. C. and J. G.), HL142951-03S1 (H. C.), and HL154754-03S1 (H. C.).

Appendix A. Supplementary data

Supplementary data to this article can be found online at https://doi. org/10.1016/j.redox.2025.103570.

References

- J.H. Oak, H. Cai, Attenuation of angiotensin II signaling recouples eNOS and inhibits nonendothelial NOX activity in diabetic mice, Diabetes 56 (2007) 118–126, https://doi.org/10.2337/db06-0288.
- [2] J.H. Oak, J.Y. Youn, H. Cai, Aminoguanidine inhibits aortic hydrogen peroxide production, VSMC NOX activity and hypercontractility in diabetic mice, Cardiovasc. Diabetol. 8 (2009) 65, https://doi.org/10.1186/1475-2840-8-65.
- [3] J.Y. Youn, L. Gao, H. Cai, The p47phox- and NADPH oxidase organiser 1 (NOXO1)-dependent activation of NADPH oxidase 1 (NOX1) mediates endothelial nitric oxide synthase (eNOS) uncoupling and endothelial dysfunction in a streptozotocin-induced murine model of diabetes, Diabetologia 55 (2012) 2069–2079, https://doi.org/10.1007/s00125-012-2557-6.
- [4] S.P. Gray, E. Di Marco, J. Okabe, C. Szyndralewiez, F. Heitz, A.C. Montezano, J. B. de Haan, C. Koulis, A. El-Osta, K.L. Andrews, et al., NADPH oxidase 1 plays a key role in diabetes mellitus-accelerated atherosclerosis, Circulation 127 (2013) 1888–1902, https://doi.org/10.1161/CIRCULATIONAHA.112.132159.
- [5] J.Y. Youn, J. Zhou, H. Cai, Bone morphogenic protein 4 mediates NOX1-dependent eNOS uncoupling, endothelial dysfunction, and COX2 induction in type 2 diabetes mellitus, Mol. Endocrinol. 29 (2015) 1123–1133, https://doi.org/10.1210/ ME.2014-1313.
- [6] Y. Zhang, P. Murugesan, K. Huang, H. Cai, NADPH oxidases and oxidase crosstalk in cardiovascular diseases: novel therapeutic targets, Nat. Rev. Cardiol. 17 (2020) 170–194, https://doi.org/10.1038/s41569-019-0260-8.
- [7] Z. Guo, Y. Zhang, C. Liu, J.Y. Youn, H. Cai, Toll-like receptor 2 (TLR2) knockout abrogates diabetic and obese phenotypes while restoring endothelial function via inhibition of NOX1, Diabetes 70 (2021) 2107–2119, https://doi.org/10.2337/ db20-0591.
- [8] L. Zhao, C.L. Zhang, L. He, Q. Chen, L. Liu, L. Kang, J. Liu, J.Y. Luo, L. Gou, D. Qu, et al., Restoration of autophagic flux improves endothelial function in diabetes through lowering mitochondrial ROS-mediated eNOS monomerization, Diabetes 71 (2022) 1099–1114. https://doi.org/10.2337/db21-0660.
- [9] K. Chalupsky, H. Cai, Endothelial dihydrofolate reductase: critical for nitric oxide bioavailability and role in angiotensin II uncoupling of endothelial nitric oxide synthase, Proc. Natl. Acad. Sci. U. S. A. 102 (2005) 9056–9061, https://doi.org/ 10.1073/pnas.0409594102.
- [10] L. Gao, K. Chalupsky, E. Stefani, H. Cai, Mechanistic insights into folic aciddependent vascular protection: dihydrofolate reductase (DHFR)-mediated

- reduction in oxidant stress in endothelial cells and angiotensin II-infused mice: a novel HPLC-based fluorescent assay for DHFR activity, J. Mol. Cell. Cardiol. 47 (2009) 752–760, https://doi.org/10.1016/j.yjmcc.2009.07.025.
- [11] M.J. Crabtree, A.B. Hale, K.M. Channon, Dihydrofolate reductase protects endothelial nitric oxide synthase from uncoupling in tetrahydrobiopterin deficiency, Free Radic. Biol. Med. 50 (2011) 1639–1646, https://doi.org/10.1016/ i.freeradbiomed.2011.03.010.
- [12] H. Li, Q. Li, Y. Zhang, W. Liu, B. Gu, T. Narumi, K.L. Siu, J.Y. Youn, P. Liu, X. Yang, et al., Novel treatment of hypertension by specifically targeting E2F for restoration of endothelial dihydrofolate reductase and eNOS function under oxidative stress, Hypertension 73 (2019) 179–189, https://doi.org/10.1161/ HYPERTENSIONAHA.118.11643.
- [13] L. Gao, K.L. Siu, K. Chalupsky, A. Nguyen, P. Chen, N.L. Weintraub, Z. Galis, H. Cai, Role of uncoupled endothelial nitric oxide synthase in abdominal aortic aneurysm formation: treatment with folic acid, Hypertension 59 (2012) 158–166, https:// doi.org/10.1161/HYPERTENSIONAHA.111.181644.
- [14] K.L. Siu, X.N. Miao, H. Cai, Recoupling of eNOS with folic acid prevents abdominal aortic aneurysm formation in angiotensin II-infused apolipoprotein E null mice, PLoS One 9 (2014) e88899, https://doi.org/10.1371/journal.pone.0088899.
- [15] X.N. Miao, K.L. Siu, H. Cai, Nifedipine attenuation of abdominal aortic aneurysm in hypertensive and non-hypertensive mice: mechanisms and implications, J. Mol. Cell. Cardiol. 87 (2015) 152–159, https://doi.org/10.1016/j.yjmcc.2015.07.031.
- [16] A. Solini, C. Rossi, E. Duranti, S. Taddei, A. Natali, A. Virdis, Saxagliptin prevents vascular remodeling and oxidative stress in db/db mice. Role of endothelial nitric oxide synthase uncoupling and cyclooxygenase, Vascul Pharmacol 76 (2016) 62–71, https://doi.org/10.1016/j.yph.2015.10.002.
- [17] E. Yamamoto, T. Nakamura, K. Kataoka, Y. Tokutomi, Y.F. Dong, M. Fukuda, H. Nako, O. Yasuda, H. Ogawa, S. Kim-Mitsuyama, Nifedipine prevents vascular endothelial dysfunction in a mouse model of obesity and type 2 diabetes, by improving eNOS dysfunction and dephosphorylation, Biochem. Biophys. Res. Commun. 403 (2010) 258–263, https://doi.org/10.1016/j.bbrc.2010.11.008.
- [18] L. Gao, Y.F. Pung, J. Zhang, P. Chen, T. Wang, M. Li, M. Meza, L. Toro, H. Cai, Sepiapterin reductase regulation of endothelial tetrahydrobiopterin and nitric oxide bioavailability, Am. J. Physiol. Heart Circ. Physiol. 297 (2009) H331–H339, https://doi.org/10.1152/ajpheart.00007.2009.
- [19] A.L. Sheehan, S. Carrell, B. Johnson, B. Stanic, B. Banfi, F.J. Miller Jr., Role for Nox1 NADPH oxidase in atherosclerosis, Atherosclerosis 216 (2011) 321–326, https://doi.org/10.1016/j.atherosclerosis.2011.02.028.
- [20] K.L. Siu, H. Cai, Circulating tetrahydrobiopterin as a novel biomarker for abdominal aortic aneurysm, Am. J. Physiol. Heart Circ. Physiol. 307 (2014) H1559–H1564, https://doi.org/10.1152/ajpheart.00444.2014.
- [21] K. Huang, Y. Wang, K.L. Siu, Y. Zhang, H. Cai, Targeting feed-forward signaling of TGFβ/NOX4/DHFR/eNOS uncoupling/TGFβ axis with anti-TGFβ and folic acid attenuates formation of aortic aneurysms: novel mechanisms and therapeutics, Redox Biol. 38 (2021) 101757, https://doi.org/10.1016/j.redox.2020.101757.
- [22] K. Huang, T. Narumi, Y. Zhang, Q. Li, P. Murugesan, Y. Wu, N.M. Liu, H. Cai, Targeting MicroRNA-192-5p, a downstream effector of NOXs (NADPH oxidases), reverses endothelial DHFR (dihydrofolate reductase) deficiency to attenuate abdominal aortic aneurysm formation, Hypertension 78 (2021) 282–293, https:// doi.org/10.1161/hypertensionaha.120.15070.
- [23] K. Huang, Y. Wu, Y. Zhang, J.Y. Youn, H. Cai, Combination of folic acid with nifedipine is completely effective in attenuating aortic aneurysm formation as a novel oral medication, Redox Biol. 58 (2022) 102521, https://doi.org/10.1016/j. redox.2022.102521.
- [24] D.E. Stec, S. Morimoto, C.D. Sigmund, Vectors for high-level expression of cDNAs controlled by tissue-specific promoters in transgenic mice, Biotechniques 31 (256–258) (2001) 260, https://doi.org/10.2144/01312bm03.
- [25] G. Gavazzi, B. Banfi, C. Deffert, L. Fiette, M. Schappi, F. Herrmann, K.H. Krause, Decreased blood pressure in NOX1-deficient mice, FEBS Lett. 580 (2006) 497–504, https://doi.org/10.1016/j.febslet.2005.12.049.
- [26] Y. Zhang, Q. Li, J.Y. Youn, H. Cai, Protein phosphotyrosine phosphatase 1B (PTP1B) in calpain-dependent feedback regulation of vascular endothelial growth factor receptor (VEGFR2) in endothelial cells: implications in vegf-dependent angiogenesis and diabetic wound healing, J. Biol. Chem. 292 (2017) 407–416, https://doi.org/10.1074/jbc.M116.766832.
- [27] K.L. Siu, Q. Li, Y. Zhang, J. Guo, J.Y. Youn, J. Du, H. Cai, NOX isoforms in the development of abdominal aortic aneurysm, Redox Biol. 11 (2017) 118–125, https://doi.org/10.1016/j.redox.2016.11.002.
- [28] Q. Li, J.Y. Youn, K.L. Siu, P. Murugesan, Y. Zhang, H. Cai, Knockout of dihydrofolate reductase in mice induces hypertension and abdominal aortic aneurysm via mitochondrial dysfunction, Redox Biol. 24 (2019) 101185, https:// doi.org/10.1016/j.redox.2019.101185.
- [29] S. Luo, A.H. Truong, A. Makino, Isolation of mouse coronary endothelial cells, J. Vis. Exp. (2016), https://doi.org/10.3791/53985.
- [30] J.Y. Youn, T. Wang, H. Cai, An ezrin/calpain/PI3K/AMPK/eNOSs1179 signaling cascade mediating VEGF-dependent endothelial nitric oxide production, Circ. Res. 104 (2009) 50–59, https://doi.org/10.1161/CIRCRESAHA.108.178467.
- [31] A. Nguyen, H. Cai, Netrin-1 induces angiogenesis via a DCC-dependent ERK1/2eNOS feed-forward mechanism, Proc. Natl. Acad. Sci. U. S. A. 103 (2006) 6530–6535, https://doi.org/10.1073/pnas.0511011103.
- [32] P. Libby, P.M. Ridker, G.K. Hansson, Progress and challenges in translating the biology of atherosclerosis, Nature 473 (2011) 317–325, https://doi.org/10.1038/ nature10146.
- [33] Y. Hattori, S. Hattori, X. Wang, H. Satoh, N. Nakanishi, K. Kasai, Oral administration of tetrahydrobiopterin slows the progression of atherosclerosis in

- apolipoprotein E-knockout mice, Arterioscler. Thromb. Vasc. Biol. 27 (2007) 865–870, https://doi.org/10.1161/01.ATV.0000258946.55438.0e.
- [34] T.S. Schmidt, E. McNeill, G. Douglas, M.J. Crabtree, A.B. Hale, J. Khoo, C. A. O'Neill, A. Cheng, K.M. Channon, N.J. Alp, Tetrahydrobiopterin supplementation reduces atherosclerosis and vascular inflammation in apolipoprotein E-knockout mice, Clin Sci (Lond). 119 (2010) 131–142, https://doi.org/10.1042/CS20090559.
- [35] C. Cunnington, T. Van Assche, C. Shirodaria, I. Kylintireas, A.C. Lindsay, J.M. Lee, C. Antoniades, M. Margaritis, R. Lee, R. Cerrato, et al., Systemic and vascular oxidation limits the efficacy of oral tetrahydrobiopterin treatment in patients with coronary artery disease, Circulation 125 (2012) 1356–1366, https://doi.org/10.1161/CIRCULATIONAHA.111.038919.
- [36] J.K. Bendall, A.C. Cave, C. Heymes, N. Gall, A.M. Shah, Pivotal role of a gp91 (phox)-containing NADPH oxidase in angiotensin II-induced cardiac hypertrophy in mice, Circulation 105 (2002) 293–296, https://doi.org/10.1161/ hc0302.103712.
- [37] E. Takimoto, H.C. Champion, M. Li, S. Ren, E.R. Rodriguez, B. Tavazzi, G. Lazzarino, N. Paolocci, K.L. Gabrielson, Y. Wang, et al., Oxidant stress from nitric oxide synthase-3 uncoupling stimulates cardiac pathologic remodeling from chronic pressure load, J. Clin. Investig. 115 (2005) 1221–1231, https://doi.org/ 10.1172/JCI21968.
- [38] J. Kuroda, T. Ago, S. Matsushima, P.Y. Zhai, M.D. Schneider, J. Sadoshima, NADPH oxidase 4 (Nox4) is a major source of oxidative stress in the failing heart, Proceedings of the National Academy of Sciences of the United States of America 107 (2010) 15565–15570, https://doi.org/10.1073/pnas.1002178107.
- [39] J. Zhang, H. Cai, Netrin-1 prevents ischemia/reperfusion-induced myocardial infarction via a DCC/ERK1/2/eNOS s1177/NO/DCC feed-forward mechanism,

- J. Mol. Cell. Cardiol. 48 (2010) 1060–1070, https://doi.org/10.1016/j. vimcc.2009.11.020.
- [40] S. Matsushima, J. Kuroda, T. Ago, P.Y. Zhai, Y. Ikeda, S. Oka, G.H. Fong, R. Tian, J. Sadoshima, Broad suppression of NADPH oxidase activity exacerbates ischemia/reperfusion injury through inadvertent downregulation of hypoxia-inducible factor-1 alpha and upregulation of peroxisome proliferator-activated receptoralpha, Circ. Res. 112 (2013) 1135, https://doi.org/10.1161/Circresaha.111.300171.
- [41] J.O. Bouhidel, P. Wang, K.L. Siu, H. Li, J.Y. Youn, H. Cai, Netrin-1 improves postinjury cardiac function in vivo via DCC/NO-dependent preservation of mitochondrial integrity, while attenuating autophagy, Biochim. Biophys. Acta 1852 (2015) 277–289, https://doi.org/10.1016/j.bbadis.2014.06.005.
- [42] K.L. Siu, C. Lotz, P. Ping, H. Cai, Netrin-1 abrogates ischemia/reperfusion-induced cardiac mitochondrial dysfunction via nitric oxide-dependent attenuation of NOX4 activation and recoupling of NOS, J. Mol. Cell. Cardiol. 78 (2015) 174–185, https://doi.org/10.1016/j.yjmcc.2014.07.005.
- [43] Q. Li, P. Wang, K. Ye, H. Cai, Central role of SIAH inhibition in DCC-dependent cardioprotection provoked by netrin-1/NO, Proc. Natl. Acad. Sci. U. S. A. 112 (2015) 899–904, https://doi.org/10.1073/pnas.1420695112.
- [44] M.C. Wendt, A. Daiber, A.L. Kleschyov, A. Mülsch, K. Sydow, E. Schulz, K. Chen, J. F. Keaney Jr., B. Lassègue, U. Walter, et al., Differential effects of diabetes on the expression of the gp91phox homologues nox1 and nox4, Free Radic. Biol. Med. 39 (2005) 381–391, https://doi.org/10.1016/j.freeradbiomed.2005.03.020.
- [45] J.Y. Youn, T. Wang, J. Blair, K.M. Laude, J.H. Oak, L.A. McCann, D.G. Harrison, H. Cai, Endothelium-specific sepiapterin reductase deficiency in DOCA-salt hypertension, Am. J. Physiol. Heart Circ. Physiol. 302 (2012) H2243–H2249, https://doi.org/10.1152/ajpheart.00835.2011.